

Observation of the decay $\psi(3686) \rightarrow \Sigma^- \bar{\Sigma}^+$ and measurement of its angular distribution

The BESIII collaboration



E-mail: besiii-publications@ihep.ac.cn

ABSTRACT: Using $(448.1 \pm 2.9) \times 10^6$ $\psi(3686)$ events collected with the BESIII detector at the BEPCII collider, the decay $\psi(3686) \rightarrow \Sigma^- \bar{\Sigma}^+$ is observed for the first time with a branching fraction of $(2.84 \pm 0.04_{\text{stat.}} \pm 0.08_{\text{sys.}}) \times 10^{-4}$, and the angular parameter α_{Σ^-} is measured to be $0.96 \pm 0.09_{\text{stat.}} \pm 0.03_{\text{sys.}}$.

KEYWORDS: Hyperon, Branching fraction, e^+e^- collision

ARXIV EPRINT: [22XX.XX](https://arxiv.org/abs/2209.14564)

Contents

1	Introduction	1
2	The BESIII detector and Monte Carlo simulation	2
3	Event selection	3
4	Measurement of the branching fraction	4
5	Measurement of the angular distribution parameter	6
6	Systematic uncertainties	6
7	Summary	8
	The BESIII Collaboration	12

1 Introduction

Two-body baryonic decays of the charmonium states J/ψ and $\psi(3686)$, here both denoted by the symbol Ψ , provide an excellent laboratory to study flavour-SU(3) symmetry breaking and test various aspects of quantum chromodynamics (QCD) in the perturbative energy regime [1].

The amplitudes of Ψ decays to different baryon octet pairs are supposed to be the same under the assumption of flavour-SU(3) symmetry. However, branching fractions are not only determined by strong interaction amplitudes, but also by electromagnetic interactions and interference between the two amplitudes [2], although these contributions are much smaller than the expected flavour-SU(3) breaking effects. With a phenomenologically plausible model [3–5], the branching fractions of Ψ decay to baryon octet final states can be described well. Perturbative QCD [6, 7] predicts the partial widths for $\psi(3686)$ decay into an exclusive hadronic state to be proportional to squares of the wave-function, which are well determined from leptonic widths. Furthermore, the ratio between the branching fractions of J/ψ and $\psi(3686)$ decays to the same final states is expected to obey the so-called “12% rule” [6, 7]. Although a large fraction of exclusive decay channels follow this rule approximately, significant violation has been observed in the $\rho\pi$ channel [8]. The ratio of the branching fraction $\mathcal{B}(\psi(3686) \rightarrow \rho\pi)$ to $\mathcal{B}(J/\psi \rightarrow \rho\pi)$ is much smaller than the perturbative QCD prediction, and this is called the “ $\rho\pi$ puzzle”. Many explanations [9] of the $\rho\pi$ puzzle have been proposed, including the J/ψ -glueball admixture scheme [10], the intrinsic-charm-component scheme [11], the sequential-fragmentation model [12], the exponential form-factor model [13], the S - D wave-mixing scheme [14, 15], the final-state

interaction scheme and others [16]. However, none of these explanations can account for all existing experimental results. Tests of the 12% rule using the baryonic decay modes are helpful in understanding the $\rho\pi$ puzzle. Experimentally, the branching fractions of Ψ decay into octet baryon pairs have been well measured, except for $\Sigma^-\bar{\Sigma}^+$ [17].

The angular distribution of a baryon pair can be written as $1 + \alpha_B \cos^2 \theta_B$, where α_B is the angular distribution parameter of the baryon, θ_B is a polar angle between the baryon and the positron beam in the centre-of-mass (c.m.) system. The value of α_B is expected to be 1 due to the helicity conservation rule [18]. In addition, in the theoretical calculations of α_B , the masses of quarks and baryons have been considered [19, 20]. Existing theoretical predictions are not consistent with the experimental measurements. The values of α_B should be the same among isospin partners, such as α_{Σ^+} and α_{Σ^0} [21, 22], α_{Ξ^0} and α_{Ξ^-} [23, 24]. There are no significant differences observed experimentally. However, the value of α_{Σ^-} has not yet been measured.

In this paper, the first observation of the decay $\psi(3686) \rightarrow \Sigma^-\bar{\Sigma}^+$ is reported, where Σ^- decays to $n\pi^-$ and $\bar{\Sigma}^+$ decays to $\bar{n}\pi^+$. The data samples used in this analysis consist of $(448.1 \pm 2.9) \times 10^6$ $\psi(3686)$ events [25] collected with the BESIII detector.

2 The BESIII detector and Monte Carlo simulation

The BESIII detector [26] records symmetric e^+e^- collisions provided by the BEPCII storage ring [27] in the c.m. energy range from 2.0 to 4.94 GeV, with a peak luminosity of $1 \times 10^{33} \text{ cm}^{-2}\text{s}^{-1}$ achieved at $\sqrt{s} = 3.77$ GeV. BESIII has collected large data samples in this energy region [28]. The cylindrical core of the BESIII detector covers 93% of the full solid angle and consists of a helium-based multilayer drift chamber (MDC), a plastic scintillator time-of-flight system (TOF), and a CsI(Tl) electromagnetic calorimeter (EMC), which are all enclosed in a superconducting solenoidal magnet providing a 1.0 T (0.9 T in 2012) magnetic field. The solenoid is supported by an octagonal flux-return yoke with resistive plate counter muon identification modules interleaved with steel. The charged-particle momentum resolution at 1 GeV/c is 0.5%, and the dE/dx resolution is 6% for electrons from Bhabha scattering. The EMC measures photon energies with a resolution of 2.5% (5%) at 1 GeV in the barrel (end-cap) region. The time resolution in the TOF barrel region is 68 ps, while that in the end-cap region is 110 ps.

Monte Carlo (MC) simulated events are used to determine the detection efficiency, optimize selection criteria, and study possible backgrounds. Simulated data samples produced with a GEANT4-based [29] package, which includes the geometric description of the BESIII detector and the detector response, are used to determine detection efficiencies and to estimate backgrounds. The simulation models the beam-energy spread and initial-state radiation (ISR) in the e^+e^- annihilations with the generator KKMC [30]. The inclusive MC sample $\psi(3686)$ includes the production of the $\psi(3686)$ resonance, the ISR production of the J/ψ , and the continuum processes incorporated in KKMC. The known decay modes are modeled with BesEvtGen [31] using branching fractions taken from the Particle Data Group (PDG) [17], and the remaining unknown charmonium decays are modelled with LUNDCHARM [32]. Final-state radiation from charged final-state particles is

incorporated using the PHOTOS package [33]. The differential cross section of the signal process ($\psi(3686) \rightarrow \Sigma^-\bar{\Sigma}^+$, $\Sigma^- \rightarrow n\pi^-$, $\bar{\Sigma}^+ \rightarrow \bar{n}\pi^+$) is expressed with respect to five observables $\xi = (\theta_{\Sigma^-}, \theta_n, \phi_n, \theta_{\bar{n}}, \phi_{\bar{n}})$, which includes four parameters α_{Σ^-} , $\Delta\Phi$, α_- and α_+ [34]. Here, θ_{Σ^-} is the polar angle between the Σ^- and the positron beam in the reaction c.m. frame, θ_n, ϕ_n and $\theta_{\bar{n}}, \phi_{\bar{n}}$ are the polar and azimuthal angles of the neutron and anti-neutron measured in the rest frames of their corresponding parent particles. The value of α_{Σ^-} is determined in this analysis, and $\Delta\Phi$ is set to be 0 by assuming no polarization. The decay asymmetry parameters α_- and α_+ in the differential cross sections are fixed to -0.068 and 0.068 using the PDG [17] values, where α_- and α_+ are used to describe the non-leptonic decays of $\Sigma^- \rightarrow n\pi^-$ and $\bar{\Sigma}^+ \rightarrow \bar{n}\pi^+$ [35]. The uncertainties in the values of these parameters are considered when assigning systematic uncertainties.

3 Event selection

The final state of the signal process is $n\pi^-\bar{n}\pi^+$. Event candidates are required to have two well-reconstructed charged tracks with zero net charge, and one anti-neutron. In order to keep the selection efficiency high there is no attempt made to reconstruct the neutron. Charged tracks detected in the MDC are required to be within a polar angle (θ) range of $|\cos\theta| < 0.93$ and θ is defined with respect to the z axis, which is along the symmetry axis of the MDC. For each charged track, the distance of closest approach to the interaction point (IP) must be less than 30 cm along the z axis, and less than 10 cm in the transverse plane. Particle identification (PID) for charged tracks combines measurements of the energy deposited in the MDC (dE/dx) and the flight time in the TOF to form likelihoods $\mathcal{L}(h)$ ($h = p, K, \pi$) for each hadron h hypothesis. Two pions are identified with the requirements that $\mathcal{L}(\pi) > \mathcal{L}(K)$ and $\mathcal{L}(\pi) > \mathcal{L}(p)$.

The anti-neutron candidates are identified using showers in the EMC. The deposited energy of each shower must be more than 600 MeV both in the barrel region ($|\cos\theta| < 0.80$) and in the end-cap region ($0.86 < |\cos\theta| < 0.92$). To exclude showers that originate from charged tracks, the angle subtended by the EMC shower and the position of the closest charged track at the EMC must be greater than 10 degrees as measured from the IP. The second moment $\sum_i E_i r_i^2 / \sum_i E_i$, where E_i is the energy deposition in the i^{th} crystal and r_i is the radial distance of the i^{th} crystal from the cluster centre, is required to be larger than 20, to suppress the photon background misidentified as anti-neutrons. To suppress electronic noise and showers unrelated to the event, the difference between the EMC time and the event start time is required to be within $[0, 700]$ ns. If the number of anti-neutron candidates in an event is more than one, the maximum deposited energy in the EMC is selected as the final event candidate.

A one-constraint kinematic fit is performed to the decay $\psi(3686) \rightarrow n\pi^-\bar{n}\pi^+$ with the constraints provided by four-momentum conservation, the invariant mass $M_{\bar{n}\pi^+}$ equal to the known $\bar{\Sigma}^+$ mass. Since the anti-neutron could annihilate with the materials in the EMC, the polar and azimuthal angles of anti-neutron are used in kinematic fit, while the deposited energy of anti-neutron are set free. Considering neutron is hardly to be detected, the three-momentum of neutron is free parameters in the kinematic fit. The χ^2 of

the kinematic fit is required to be smaller than 50, which is a value optimized by using the figure-of-merit $S/\sqrt{S+B}$, where S is the number of signal MC events and B is the number of the estimated background events. To suppress background from $\psi(3686) \rightarrow \pi^+\pi^-J/\psi$ decays, with $J/\psi \rightarrow n\bar{n}$, the recoil mass of the $\pi^+\pi^-$ pair is required to be less than 2.9 GeV/ c^2 .

An inclusive MC sample of 506 million $\psi(3686)$ events is used to study possible background channels, with a generic event-type analysis tool, TopoAna [36]. The potential sources of peaking background are found to be $\psi(3686) \rightarrow \gamma\chi_{cJ}(\chi_{cJ} \rightarrow \Sigma^-\bar{\Sigma}^+)$ ($J=0,1,2$) and $\psi(3686) \rightarrow \gamma\eta_c(\eta_c \rightarrow \Sigma^-\bar{\Sigma}^+)$, and $\psi(3686) \rightarrow \pi^0\Sigma^-\bar{\Sigma}^+$. To estimate the sizes and distributions of these background processes, samples of 100 million events are generated for each channel. In these, the decay processes $\psi(3686) \rightarrow \gamma\chi_{cJ}(\chi_{cJ} \rightarrow \Sigma^-\bar{\Sigma}^+)$, $\psi(3686) \rightarrow \gamma\eta_c(\eta_c \rightarrow \Sigma^-\bar{\Sigma}^+)$, and $\psi(3686) \rightarrow \pi^0\Sigma^-\bar{\Sigma}^+$ are generated with the P2GCJ ($J=0,1,2$), JPE, and phase-space models. When accounting for the branching fractions [17] and detection efficiencies of these decays, the numbers of background events passing the selection in the data sample are predicted to be 562 ± 86 for $\psi(3686) \rightarrow \gamma\chi_{cJ}(\chi_{cJ} \rightarrow \Sigma^-\bar{\Sigma}^+)$ and 5 ± 1 for $\psi(3686) \rightarrow \gamma\eta_c(\eta_c \rightarrow \Sigma^-\bar{\Sigma}^+)$. The contribution of $\psi(3686) \rightarrow \pi^0\Sigma^-\bar{\Sigma}^+$ decays is negligible.

An off-resonance data sample taken at the c.m. energy of 3.65 GeV is used to estimate the non- $\psi(3686)$ background. The size of this contribution, $N_{\text{non-}\psi(3686)}$, is determined according to the formula: $N_{\text{non-}\psi(3686)} = N_{\text{cont}}^{\text{obs}} \cdot \frac{L_{\psi(3686)}}{L_{\text{cont}}} \cdot \frac{s_{\text{cont}}}{s_{\psi(3686)}} \cdot \frac{\varepsilon_{\text{cont}}}{\varepsilon_{\psi(3686)}} = 92 \pm 53$ events, where $N_{\text{cont}}^{\text{obs}} = 7 \pm 4$ is the number of events surviving the same selection criteria when applied to the 3.65 GeV sample, s_{cont} and $s_{\psi(3686)}$ are the squares of the c.m. energies at 3.65 GeV and 3.686 GeV, $\varepsilon_{\text{cont}} = 5.96\%$ and $\varepsilon_{\psi(3686)} = 5.26\%$ are the selection efficiencies at 3.65 GeV and 3.686 GeV, and $L_{\text{cont}} = 44 \text{ pb}^{-1}$ and $L_{\psi(3686)} = 668.55 \text{ pb}^{-1}$ and are the integrated luminosities at 3.65 GeV and 3.686 GeV, respectively.

4 Measurement of the branching fraction

The Σ^- candidate is reconstructed from the π^- and the missing neutron. To determine the number of signal events, an unbinned maximum likelihood fit is performed to the distribution of the invariant mass $n\pi^-$ ($M_{n\pi^-}$) in the region of [1.15, 1.25] GeV/ c^2 . The signal is described by the shape found in the MC simulations, convoluted with a Gaussian function which accommodates any difference in mass resolution between data and MC simulations. The peaking background is described with the shapes of the MC-simulated exclusive background channels, and the corresponding numbers of events are fixed to the estimated values. The non-peaking background is described with a second-order polynomial function. Figure 1 shows the fit of the $n\pi^-$ mass distribution. The χ^2/ndf of the fit is 35.64/44, where ndf is the number of degrees of freedom.

The branching fraction is calculated according to

$$Br = \frac{N_{\text{sig}} - N_{\text{non-}\psi(3686)}}{\varepsilon \times \prod Br_i \times N_{\text{tot}}}, \quad (4.1)$$

where N_{sig} is the number of signal events and $N_{\text{non-}\psi(3686)}$ is the number of non- $\psi(3686)$ events, $\prod Br_i$ is the product of the branching fractions of the intermediate states, and N_{tot} is the total number of $\psi(3686)$ events [25]. The detection efficiency ε is estimated from the signal MC simulations. Differences in detection efficiency between data and MC simulations is accounted for using control samples of $J/\psi \rightarrow p\bar{p}\pi^+\pi^-$, $J/\psi \rightarrow p\bar{n}\pi^-$, and $\psi(3686) \rightarrow p\bar{n}\pi^-$ decays. Here, in order to study the difference of anti-neutron efficiency from EMC and kinematic fit, the anti-neutron efficiency ratios between data and MC simulations are determined with different anti-neutron momentum and polar-angle regions. Besides, the efficiency difference, the polar and azimuth angles of anti-neutron, and their error matrices have been corrected based on the data-driven method [37]. The π^+ and π^- efficiency ratios are also determined using the same method. The branching fraction is calculated to be $(2.84 \pm 0.04) \times 10^{-4}$, where the uncertainty is statistical only. The corresponding number of signal events, non- $\psi(3686)$ events, detection efficiency after correcting for data-MC differences, and branching fraction are listed in Tab. 1.

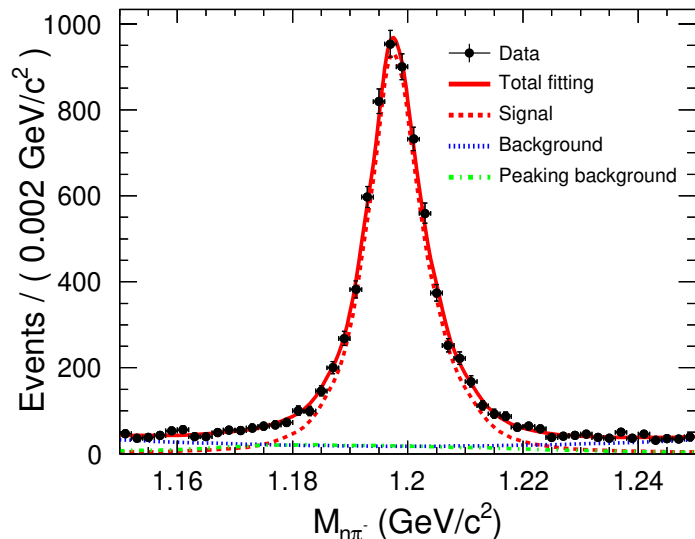


Figure 1. The distribution of $M_{n\pi^-}$ for the signal process $\psi(3686) \rightarrow \Sigma^-\bar{\Sigma}^+$, $\Sigma^- \rightarrow n\pi^-$, $\bar{\Sigma}^+ \rightarrow \bar{n}\pi^+$. The black dots with error bars are the data, the red solid line is the total fit function, the red dashed line is the signal function, the blue dotted line is the non-peaking background function, and the green dash-dotted line is the peaking background function.

Table 1. The number of signal events, the number of non- $\psi(3686)$ background events and the detection efficiency.

Channel	N_{sig}	$N_{\text{non-}\psi(3686)}$	ε
$\psi(3686) \rightarrow \Sigma^-\bar{\Sigma}^+$	6765 ± 106	92 ± 53	5.26%

5 Measurement of the angular distribution parameter

To determine the value of the angular parameter α_{Σ^-} , a least-squares fit is performed to the $\cos\theta_{\Sigma^-}$ distribution in the range of $[-1, 1]$. The numbers of signal events are determined in ten equally sized intervals of $\cos\theta_{\Sigma^-}$ with the same method as used in the branching fraction measurement. The detection efficiency in each interval is determined with MC simulations, which is then corrected to account for data-MC differences. The $\cos\theta_{\Sigma^-}$ distribution after efficiency correction is shown in Fig. 2. Superimposed is the result of a fit to the function $1 + \alpha_{\Sigma^-} \cos^2\theta_{\Sigma^-}$. The parameter α_{Σ^-} is measured to be 0.96 ± 0.09 , where the uncertainty is statistical, and its lower limit is determined to be larger than 0.835 at 90% confidence level. The χ^2/ndf of the fit is 13.52/8, where ndf is the number of degrees of freedom.

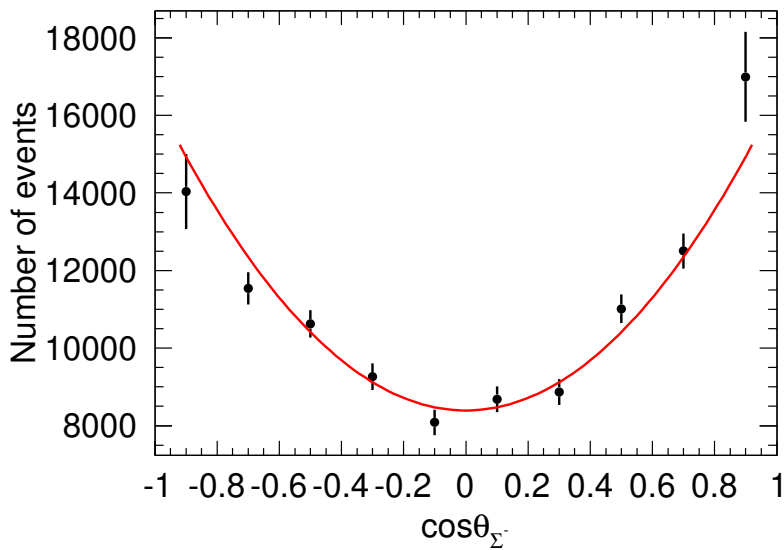


Figure 2. The angular distribution for the signal process $\psi(3686) \rightarrow \Sigma^- \bar{\Sigma}^+$, $\Sigma^- \rightarrow n\pi^-$, $\bar{\Sigma}^+ \rightarrow \bar{n}\pi^+$. The black dots with error bars indicate the signal yields after efficiency correction, and the red curve represents the fit function.

6 Systematic uncertainties

To estimate the systematic uncertainties in the measurement of the branching fraction, we consider the differences of the detection efficiency and resolution between data and MC simulations, the uncertainty associated with the generator models, the background estimations and other sources. An overview of all the systematic uncertainties on the branching fraction measurement is given in Tab. 2.

The tracking and PID efficiency in MC simulations is corrected in bins of transverse momentum and polar angle to agree with that measured in data. The uncertainty on these corrections, derived from the control channels and averaged over bins, is assigned as a systematic uncertainty on the branching fraction. For charged tracks the study is performed with a control sample of $J/\psi \rightarrow p\bar{p}\pi^+\pi^-$ events, and the relative uncertainty is found to be 0.2%. The relative uncertainty for the reconstruction of the anti-neutron

Table 2. Systematic uncertainties on the branching fraction measurement (%).

Source	Uncertainty (%)
MC efficiency correction	1.9
Decay parameter	1.2
QED peaking-background estimation	0.8
Non-peaking background estimation	0.4
Peaking-background estimation	0.2
Kinematic fitting	0.2
Total number of $\psi(3686)$	0.7
Total	2.5

is set with control samples of $J/\psi \rightarrow p\bar{n}\pi^-$ and $\psi(3686) \rightarrow p\bar{n}\pi^-$ events and found to be 1.9%. Hence, the total systematic uncertainty associated with the MC efficiency correction is 1.9%.

In the signal generator model [34], the values of α_- and α_+ are set to be -0.068 and 0.068 for Σ^- and $\bar{\Sigma}^+$ respectively. Furthermore, we assume that there is no polarization by setting $\Delta\Phi$ to 0. To evaluate the systematic uncertainty associated with these assumptions, we vary α_- and α_+ by one standard deviation (0.008), and change $\Delta\Phi$ to be $-\pi$ or $+\pi$. We compare the efficiencies after these variations with the baseline efficiency, and take the maximum difference, 1.2%, as the corresponding systematic uncertainty.

Possible systematic effects due to the requirement of $M_{\text{rec}}(\pi^+\pi^-) < 2.9 \text{ GeV}/c^2$ are investigated by varying the selection criteria between 2.80 and 2.91 GeV/c^2 in steps of 1 MeV/c^2 . The variations observed are compatible with statistical fluctuations and thus no uncertainty is assigned associated with this requirement [38].

The uncertainty associated with non-peaking background is estimated by changing the order of polynomial function used to describe this background. The difference of 0.4% with respect to the baseline configuration is taken as the systematic uncertainty arising from this source. The uncertainties associated with the number of non- $\psi(3686)$ background events and the peaking background are assigned by varying the sizes of these backgrounds by one standard deviation, giving contributions of 0.8% and 0.2%, respectively.

To estimate the size of any potential bias arising from the kinematic fit, we obtain the χ^2 distributions with the track correction method for the helix parameters that are corrected to reduce the differences between data and MC simulations [39]. Besides, the polar and azimuth angles and error matrix of anti-neutron in kinematic fit have also been corrected [37]. Compared with the baseline value, the difference of 0.2% is taken as the systematic uncertainty. An uncertainty of 0.7% is assigned to reflect the knowledge of the number of $\psi(3686)$ events in the sample, which is measured from inclusive hadronic decays, as described in Ref. [25].

The main sources of systematic uncertainty on baryonic angular distribution measurement are associated with knowledge of the signal yields, the efficiency correction, and the fitting process. An overview of all the systematic uncertainties is given in Tab. 3.

Table 3. Systematic uncertainties of angular-distribution measurement (%).

Source	Uncertainty(%)
MC efficiency correction	0.5
QED peaking background estimation	negligible
Non-peaking background estimation	1.4
Peaking background estimation	1.6
Kinematic fitting	0.3
Number of bins	0.4
Fitting $\cos\theta_{\Sigma^-}$ range	1.9
Total	2.9

In the angular distribution measurement, the number of signal events in each bin is determined by the same method as for the branching fraction measurement. The uncertainties on this yield determination are associated with the MC efficiency correction, background estimation and kinematic-fitting requirement. These uncertainties are estimated with the same method as for the branching fraction. In doing this, we consider the correlations between the measurements in each bin. We then re-perform the fit to the angular distribution and take the difference with respect to baseline value as the systematic uncertainty for each contribution. The uncertainties associated with the α_{Σ^-} fit itself are estimated by varying the fitting range in $\cos\theta_{\Sigma^-}$ from $[-1.0, 1.0]$ to $[-0.8, 0.8]$, and also changing the number of bins from ten to eight. In both cases the changes in result are assigned as contributions to the uncertainties. The total systematic uncertainty on α_{Σ^-} is 0.029.

7 Summary

In summary, based on the $(448.1 \pm 2.9) \times 10^6$ $\psi(3686)$ events collected at BESIII detector, the branching fraction and angular parameter, α_{Σ^-} , of $\psi(3686) \rightarrow \Sigma^- \bar{\Sigma}^+$ decays are measured for the first time. The measurements yield $(2.84 \pm 0.04_{\text{stat.}} \pm 0.08_{\text{syst.}}) \times 10^{-4}$ for the branching fraction and $\alpha_{\Sigma^-} = 0.96 \pm 0.09_{\text{stat.}} \pm 0.03_{\text{syst.}}$. Table 4 summarizes measurements of the angular parameter and branching fraction for $\psi(3686) \rightarrow \Sigma^+ \bar{\Sigma}^-$, $\Sigma^0 \bar{\Sigma}^0$, and $\Sigma^- \bar{\Sigma}^+$ channels, and predicted values for the branching fractions. The measured branching fraction is around 2.4σ above the theoretical prediction value $(2.46 \pm 0.13) \times 10^{-4}$ [5]. There are significant differences between the value of α_{Σ^-} and those of its isospin partners α_{Σ^+} and α_{Σ^0} , which are worthy of further investigation. Finally, it is noted that the analysis method pursued here can also be used to measure the branching fraction of $J/\psi \rightarrow \Sigma^- \bar{\Sigma}^+$, which in combination with the result reported in this paper will provide an opportunity to further test the “12% rule” in charmonium decays.

Acknowledgments

The BESIII collaboration thanks the staff of BEPCII and the IHEP computing center for their strong support. This work is supported in part by National Key R&D Program

Table 4. Summary of the measured angular parameters and branching fractions of $\psi(3686) \rightarrow \Sigma^+\bar{\Sigma}^-, \Sigma^0\bar{\Sigma}^0$, and $\Sigma^-\bar{\Sigma}^+$, together with theoretical predictions of the branching fractions.

Decay mode	Br($\times 10^{-4}$)	Angular parameter α_B	Br prediction($\times 10^{-4}$) [5]
$\psi(3686) \rightarrow \Sigma^+\bar{\Sigma}^-$	$2.43 \pm 0.03 \pm 0.05$ [40]	$0.682 \pm 0.030 \pm 0.011$ [21]	2.29 ± 0.15
$\psi(3686) \rightarrow \Sigma^0\bar{\Sigma}^0$	$2.44 \pm 0.03 \pm 0.11$ [22]	$0.71 \pm 0.11 \pm 0.04$ [22]	2.37 ± 0.09
$\psi(3686) \rightarrow \Sigma^-\bar{\Sigma}^+$	$2.84 \pm 0.04 \pm 0.08$	$0.96 \pm 0.09 \pm 0.03$	2.46 ± 0.13

of China under Contracts Nos. 2020YFA0406300, 2020YFA0406400; National Natural Science Foundation of China (NSFC) under Contracts Nos. 11635010, 11735014, 11835012, 11935015, 11935016, 11935018, 11961141012, 12022510, 12025502, 12035009, 12035013, 12192260, 12192261, 12192262, 12192263, 12192264, 12192265; the Chinese Academy of Sciences (CAS) Large-Scale Scientific Facility Program; Joint Large-Scale Scientific Facility Funds of the NSFC and CAS under Contract No. U1832207; the CAS Center for Excellence in Particle Physics (CCEPP); 100 Talents Program of CAS; The Institute of Nuclear and Particle Physics (INPAC) and Shanghai Key Laboratory for Particle Physics and Cosmology; Sponsored by Shanghai Pujiang Program(20PJ1401700); ERC under Contract No. 758462; European Union’s Horizon 2020 research and innovation programme under Marie Skłodowska-Curie grant agreement under Contract No. 894790; German Research Foundation DFG under Contracts Nos. 443159800, Collaborative Research Center CRC 1044, GRK 2149; Istituto Nazionale di Fisica Nucleare, Italy; Ministry of Development of Turkey under Contract No. DPT2006K-120470; National Science and Technology fund; National Science Research and Innovation Fund (NSRF) via the Program Management Unit for Human Resources & Institutional Development, Research and Innovation under Contract No. B16F640076; STFC (United Kingdom); Suranaree University of Technology (SUT), Thailand Science Research and Innovation (TSRI), and National Science Research and Innovation Fund (NSRF) under Contract No. 160355; The Royal Society, UK under Contracts Nos. DH140054, DH160214; The Swedish Research Council; U. S. Department of Energy under Contract No. DE-FG02-05ER41374.

References

- [1] G.R. Farrar and R. D. Jackson, *Phys. Rev. Lett.* **35**, 1416 (1975); B. L. Ioffe, *Phys. Lett. B* **63**, 425 (1976); A. I. Vainshtein and V. I. Zakharov, *Phys. Lett. B* **72**, 368 (1978); S. J. Brodsky and G. P. Lepage, *Phys. Rev. D* **24**, 2848 (1981).
- [2] S. Rudaz, *Phys. Rev. D* **14**, 298 (1976).
- [3] K. Zhu, X. H. Mo and C. Z. Yuan, *Int. J. Mod. Phys. A* **30**, 1550148 (2015).
- [4] R. B. Ferroli, A. Mangoni, S. Pacetti and K. Zhu, *Phys. Lett. B* **799**, 135041 (2019).
- [5] R. B. Ferroli, A. Mangoni, S. Pacetti and K. Zhu, *Phys. Rev. D* **103**, 016005 (2021).
- [6] T. Appelquist and H. D. Politzer, *Phys. Rev. Lett.* **34**, 43 (1975).
- [7] A. De Rujula and S. L. Glashow, *Phys. Rev. Lett.* **34**, 46 (1975).

- [8] M. E. B. Franklin, G. J. Feldman, G. S. Abrams, M. S. Alam, C. A. Blocker, A. Blondel, A. Boyarski, M. Breidenbach, D. L. Burke and W. C. Carithers, *et al.* [Phys. Rev. Lett.](#) **51**, 963 (1983).
- [9] X. H. Mo, C. Z. Yuan and P. Wang, [Chin. Phys. C](#) **31**, 686 (2007).
- [10] G. Li, Q. Zhao and C. H. Chang, [J. Phys. G](#) **35**, 055002 (2008).
- [11] S. J. Brodsky and M. Karliner, [Phys. Rev. Lett.](#) **78**, 4682 (1997).
- [12] G. Karl and W. Roberts, [Phys. Lett. B](#) **144**, 263 (1984).
- [13] M. Chaichian and N. A. Tornqvist, [Nucl. Phys. B](#) **323**, 75 (1989).
- [14] K. Y. Liu and K. T. Chao, [Phys. Rev. D](#) **70**, 094001 (2004).
- [15] J. L. Rosner, [Phys. Rev. D](#) **64**, 094002 (2001).
- [16] X. Q. Li, D. V. Bugg and B. S. Zou, [Phys. Rev. D](#) **55**, 1421 (1997).
- [17] P.A. Zyla *et al.* (Particle Data Group), [PTEP](#) **2022**, 083C01 (2022).
- [18] S. J. Brodsky and G. P. Lepage, [Phys. Rev. D](#) **24**, 2848 (1981).
- [19] M. Claudson, S. L. Glashow and M. B. Wise, [Phys. Rev. D](#) **25**, 1345 (1982).
- [20] C. Carimalo, [Int. J. Mod. Phys. A](#) **2**, 249 (1987).
- [21] M. Ablikim *et al.* (BESIII Collaboration), [Phys. Rev. Lett.](#) **125**, 052004 (2020).
- [22] M. Ablikim *et al.* (BESIII Collaboration), [Phys. Rev. D](#) **95**, 052003 (2017).
- [23] M. Ablikim *et al.* (BESIII Collaboration), [Phys. Lett. B](#) **770**, 217 (2017).
- [24] M. Ablikim *et al.* (BESIII Collaboration), [Phys. Rev. D](#) **93**, 072003 (2016).
- [25] M. Ablikim *et al.* (BESIII Collaboration), [Chin. Phys. C](#) **42**, 023001 (2018).
- [26] M. Ablikim *et al.* (BESIII Collaboration), [Nucl. Instrum. Meth. A](#) **614**, 345 (2010).
- [27] C. H. Yu *et al.*, Proceedings of IPAC2016, Busan, Korea, 2016, [doi:10.18429/JACoW-IPAC2016-TUYA01](https://doi.org/10.18429/JACoW-IPAC2016-TUYA01).
- [28] M. Ablikim *et al.* (BESIII Collaboration), [Chin. Phys. C](#) **44**, 040001 (2020).
- [29] S. Agostinelli *et al.* (GEANT4 Collaboration), [Nucl. Instrum. Meth. A](#) **506**, 250 (2003); J. Allison *et al.*, [IEEE Trans. Nucl. Sci.](#) **53**, 270 (2006); J. Allison *et al.*, [Nucl. Instrum. Meth. A](#) **835**, 186 (2016).
- [30] S. Jadach, B. F. L. Ward and Z. Was, [Comp. Phys. Commu.](#) **130**, 260 (2000); [Phys. Rev. D](#) **63**, 113009 (2001).
- [31] D. J. Lange, [Nucl. Instrum. Meth. A](#) **462**, 152 (2001); R. G. Ping, [Chin. Phys. C](#) **32**, 599 (2008).
- [32] J. C. Chen, G. S. Huang, X. R. Qi, D. H. Zhang and Y. S. Zhu, [Phys. Rev. D](#) **62**, 034003 (2000); R. L. Yang, R. G. Ping and H. Chen, [Chin. Phys. Lett.](#) **31**, 061301 (2014).
- [33] E. Barberio, B. van Eijk and Z. Was, [Comput. Phys. Commun.](#) **66**, 115 (1991); E. Richter-Was, [Phys. Lett. B](#) **303**, 163 (1993); P. Golonka and Z. Was, [Eur. Phys. J. C](#) **45**, 97 (2006).
- [34] G. Fäldt and A. Kupsc, [Phys. Lett. B](#) **772**, 16 (2017).
- [35] T. D. Lee and C. N. Yang, [Phys. Rev.](#) **108**, 1645 (1957).

- [36] X. Y. Zhou, S. X. Du, G. Li and C. P. Shen, [Comput. Phys. Commun.](#) **258**, 107540 (2021).
- [37] L. Liu, X. R. Zhou and H. P. Peng, [Nucl. Instrum. Meth. A](#) **1033**, 166672 (2022).
- [38] R. Barlow, [[arXiv:hep-ex/0207026](#) [hep-ex]].
- [39] M. Ablikim *et al.* (BESIII Collaboration), [Phys. Rev. D](#) **87**, 012002 (2013).
- [40] M. Ablikim *et al.* (BESIII Collaboration), [JHEP](#) **11**, 226 (2021).

The BESIII Collaboration

M. Ablikim¹, M. N. Achasov^{11,b}, P. Adlarson⁷⁰, M. Albrecht⁴, R. Aliberti³¹, A. Amoroso^{69A,69C}, M. R. An³⁵, Q. An^{66,53}, X. H. Bai⁶¹, Y. Bai⁵², O. Bakina³², R. Baldini Ferroli^{26A}, I. Balossino^{27A}, Y. Ban^{42,g}, V. Batozskaya^{1,40}, D. Becker³¹, K. Begzsuren²⁹, N. Berger³¹, M. Bertani^{26A}, D. Bettoni^{27A}, F. Bianchi^{69A,69C}, J. Bloms⁶³, A. Bortone^{69A,69C}, I. Boyko³², R. A. Briere⁵, A. Brueggemann⁶³, H. Cai⁷¹, X. Cai^{1,53}, A. Calcaterra^{26A}, G. F. Cao^{1,58}, N. Cao^{1,58}, S. A. Cetin^{57A}, J. F. Chang^{1,53}, W. L. Chang^{1,58}, G. Chelkov^{32,a}, C. Chen³⁹, Chao Chen⁵⁰, G. Chen¹, H. S. Chen^{1,58}, M. L. Chen^{1,53}, S. J. Chen³⁸, S. M. Chen⁵⁶, T. Chen¹, X. R. Chen^{28,58}, X. T. Chen¹, Y. B. Chen^{1,53}, Z. J. Chen^{23,h}, W. S. Cheng^{69C}, S. K. Choi⁵⁰, X. Chu³⁹, G. Cibinetto^{27A}, F. Cossio^{69C}, J. J. Cui⁴⁵, H. L. Dai^{1,53}, J. P. Dai⁷³, A. Dbeyssi¹⁷, R. E. de Boer⁴, D. Dedovich³², Z. Y. Deng¹, A. Denig³¹, I. Denysenko³², M. Destefanis^{69A,69C}, F. De Mori^{69A,69C}, Y. Ding³⁶, J. Dong^{1,53}, L. Y. Dong^{1,58}, M. Y. Dong^{1,53,58}, X. Dong⁷¹, S. X. Du⁷⁵, P. Egorov^{32,a}, Y. L. Fan⁷¹, J. Fang^{1,53}, S. S. Fang^{1,58}, W. X. Fang¹, Y. Fang¹, R. Farinelli^{27A}, L. Fava^{69B,69C}, F. Feldbauer⁴, G. Felici^{26A}, C. Q. Feng^{66,53}, J. H. Feng⁵⁴, K. Fischer⁶⁴, M. Fritsch⁴, C. Fritsch⁶³, C. D. Fu¹, H. Gao⁵⁸, Y. N. Gao^{42,g}, Yang Gao^{66,53}, S. Garbolino^{69C}, I. Garzia^{27A,27B}, P. T. Ge⁷¹, Z. W. Ge³⁸, C. Geng⁵⁴, E. M. Gersabeck⁶², A. Gilman⁶⁴, K. Goetzen¹², L. Gong³⁶, W. X. Gong^{1,53}, W. Gradl³¹, M. Greco^{69A,69C}, L. M. Gu³⁸, M. H. Gu^{1,53}, Y. T. Gu¹⁴, C. Y. Guan^{1,58}, A. Q. Guo^{28,58}, L. B. Guo³⁷, R. P. Guo⁴⁴, Y. P. Guo^{10,f}, A. Guskov^{32,a}, T. T. Han⁴⁵, W. Y. Han³⁵, X. Q. Hao¹⁸, F. A. Harris⁶⁰, K. K. He⁵⁰, K. L. He^{1,58}, F. H. Heinsius⁴, C. H. Heinz³¹, Y. K. Heng^{1,53,58}, C. Herold⁵⁵, M. Himmelreich^{31,d}, G. Y. Hou^{1,58}, Y. R. Hou⁵⁸, Z. L. Hou¹, H. M. Hu^{1,58}, J. F. Hu^{51,i}, T. Hu^{1,53,58}, Y. Hu¹, G. S. Huang^{66,53}, K. X. Huang⁵⁴, L. Q. Huang^{28,58}, X. T. Huang⁴⁵, Y. P. Huang¹, Z. Huang^{42,g}, T. Hussain⁶⁸, N. Hüsken^{25,31}, W. Imoehl²⁵, M. Irshad^{66,53}, J. Jackson²⁵, S. Jaeger⁴, S. Janchiv²⁹, E. Jang⁵⁰, J. H. Jeong⁵⁰, Q. Ji¹, Q. P. Ji¹⁸, X. B. Ji^{1,58}, X. L. Ji^{1,53}, Y. Y. Ji⁴⁵, Z. K. Jia^{66,53}, H. B. Jiang⁴⁵, S. S. Jiang³⁵, X. S. Jiang^{1,53,58}, Y. Jiang⁵⁸, J. B. Jiao⁴⁵, Z. Jiao²¹, S. Jin³⁸, Y. Jin⁶¹, M. Q. Jing^{1,58}, T. Johansson⁷⁰, N. Kalantar-Nayestanaki⁵⁹, X. S. Kang³⁶, R. Kappert⁵⁹, M. Kavatsyuk⁵⁹, B. C. Ke⁷⁵, I. K. Keshk⁴, A. Khokkaz⁶³, R. Kiuchi¹, R. Kliemt¹², L. Koch³³, O. B. Kolcu^{57A}, B. Kopf⁴, M. Kuemmel⁴, M. Kuessner⁴, A. Kupsc^{40,70}, W. Kühn³³, J. J. Lane⁶², J. S. Lange³³, P. Larin¹⁷, A. Lavanaia²⁴, L. Lavezzi^{69A,69C}, Z. H. Lei^{66,53}, H. Leithoff³¹, M. Lellmann³¹, T. Lenz³¹, C. Li⁴³, C. Li³⁹, C. H. Li³⁵, Cheng Li^{66,53}, D. M. Li⁷⁵, F. Li^{1,53}, G. Li¹, H. Li^{66,53}, H. Li⁴⁷, H. B. Li^{1,58}, H. J. Li¹⁸, H. N. Li^{51,i}, J. Q. Li⁴, J. S. Li⁵⁴, J. W. Li⁴⁵, Ke Li¹, L. J. Li¹, L. K. Li¹, Lei Li³, M. H. Li³⁹, P. R. Li^{34,j,k}, S. X. Li¹⁰, S. Y. Li⁵⁶, T. Li⁴⁵, W. D. Li^{1,58}, W. G. Li¹, X. H. Li^{66,53}, X. L. Li⁴⁵, Xiaoyu Li^{1,58}, Y. G. Li^{42,g}, Z. X. Li¹⁴, H. Liang³⁰, H. Liang^{1,58}, H. Liang^{66,53}, Y. F. Liang⁴⁹, Y. T. Liang^{28,58}, G. R. Liao¹³, L. Z. Liao⁴⁵, J. Libby²⁴, A. Limphirat⁵⁵, C. X. Lin⁵⁴, D. X. Lin^{28,58}, T. Lin¹, B. J. Liu¹, C. X. Liu¹, D. Liu^{17,66}, F. H. Liu⁴⁸, Fang Liu¹, Feng Liu⁶, G. M. Liu^{51,i}, H. Liu^{34,j,k}, H. B. Liu¹⁴, H. M. Liu^{1,58}, Huanhuan Liu¹, Huihui Liu¹⁹, J. B. Liu^{66,53}, J. L. Liu⁶⁷, J. Y. Liu^{1,58}, K. Liu¹, K. Y. Liu³⁶, Ke Liu²⁰, L. Liu^{66,53}, Lu Liu³⁹, M. H. Liu^{10,f}, P. L. Liu¹, Q. Liu⁵⁸, S. B. Liu^{66,53}, T. Liu^{10,f}, W. K. Liu³⁹, W. M. Liu^{66,53}, X. Liu^{34,j,k}, Y. Liu^{34,j,k}, Y. B. Liu³⁹, Z. A. Liu^{1,53,58}, Z. Q. Liu⁴⁵, X. C. Lou^{1,53,58}, F. X. Lu⁵⁴, H. J. Lu²¹, J. G. Lu^{1,53}, X. L. Lu¹, Y. Lu⁷, Y. P. Lu^{1,53}, Z. H. Lu¹, C. L. Luo³⁷, M. X. Luo⁷⁴, T. Luo^{10,f}, X. L. Luo^{1,53}, X. R. Lyu⁵⁸, Y. F. Lyu³⁹, F. C. Ma³⁶, H. L. Ma¹, L. L. Ma⁴⁵, M. M. Ma^{1,58}, Q. M. Ma¹, R. Q. Ma^{1,58}, R. T. Ma⁵⁸, X. Y. Ma^{1,53}, Y. Ma^{42,g}, F. E. Maas¹⁷, M. Maggiora^{69A,69C}, S. Maldaner⁴, S. Malde⁶⁴, Q. A. Malik⁶⁸, A. Mangoni^{26B}, Y. J. Mao^{42,g}, Z. P. Mao¹, S. Marcello^{69A,69C}, Z. X. Meng⁶¹,

G. Mezzadri^{27A}, H. Miao¹, T. J. Min³⁸, R. E. Mitchell²⁵, X. H. Mo^{1,53,58}, N. Yu. Muchnoi^{11,b}, Y. Nefedov³², F. Nerling^{17,d}, I. B. Nikolaev^{11,b}, Z. Ning^{1,53}, S. Nisar^{9,l}, Y. Niu⁴⁵, S. L. Olsen⁵⁸, Q. Ouyang^{1,53,58}, S. Pacetti^{26B,26C}, X. Pan^{10,f}, Y. Pan⁵², A. Pathak³⁰, M. Pelizaesus⁴, H. P. Peng^{66,53}, K. Peters^{12,d}, J. L. Ping³⁷, R. G. Ping^{1,58}, S. Plura³¹, S. Pogodin³², V. Prasad^{66,53}, F. Z. Qi¹, H. Qi^{66,53}, H. R. Qi⁵⁶, M. Qi³⁸, T. Y. Qi^{10,f}, S. Qian^{1,53}, W. B. Qian⁵⁸, Z. Qian⁵⁴, C. F. Qiao⁵⁸, J. J. Qin⁶⁷, L. Q. Qin¹³, X. P. Qin^{10,f}, X. S. Qin⁴⁵, Z. H. Qin^{1,53}, J. F. Qiu¹, S. Q. Qu⁵⁶, K. H. Rashid⁶⁸, C. F. Redmer³¹, K. J. Ren³⁵, A. Rivetti^{69C}, V. Rodin⁵⁹, M. Rolo^{69C}, G. Rong^{1,58}, Ch. Rosner¹⁷, S. N. Ruan³⁹, H. S. Sang⁶⁶, A. Sarantsev^{32,c}, Y. Schelhaas³¹, C. Schnier⁴, K. Schoenning⁷⁰, M. Scodreggio^{27A,27B}, K. Y. Shan^{10,f}, W. Shan²², X. Y. Shan^{66,53}, J. F. Shangguan⁵⁰, L. G. Shao^{1,58}, M. Shao^{66,53}, C. P. Shen^{10,f}, H. F. Shen^{1,58}, X. Y. Shen^{1,58}, B. A. Shi⁵⁸, H. C. Shi^{66,53}, J. Y. Shi¹, Q. Q. Shi⁵⁰, R. S. Shi^{1,58}, X. Shi^{1,53}, X. D Shi^{66,53}, J. J. Song¹⁸, W. M. Song^{30,1}, Y. X. Song^{42,g}, S. Sosio^{69A,69C}, S. Spataro^{69A,69C}, F. Stieler³¹, K. X. Su⁷¹, P. P. Su⁵⁰, Y. J. Su⁵⁸, G. X. Sun¹, H. Sun⁵⁸, H. K. Sun¹, J. F. Sun¹⁸, L. Sun⁷¹, S. S. Sun^{1,58}, T. Sun^{1,58}, W. Y. Sun³⁰, X Sun^{23,h}, Y. J. Sun^{66,53}, Y. Z. Sun¹, Z. T. Sun⁴⁵, Y. H. Tan⁷¹, Y. X. Tan^{66,53}, C. J. Tang⁴⁹, G. Y. Tang¹, J. Tang⁵⁴, L. Y. Tao⁶⁷, Q. T. Tao^{23,h}, M. Tat⁶⁴, J. X. Teng^{66,53}, V. Thoren⁷⁰, W. H. Tian⁴⁷, Y. Tian^{28,58}, I. Uman^{57B}, B. Wang¹, B. L. Wang⁵⁸, C. W. Wang³⁸, D. Y. Wang^{42,g}, F. Wang⁶⁷, H. J. Wang^{34,j,k}, H. P. Wang^{1,58}, K. Wang^{1,53}, L. L. Wang¹, M. Wang⁴⁵, M. Z. Wang^{42,g}, Meng Wang^{1,58}, S. Wang¹³, S. Wang^{10,f}, T. Wang^{10,f}, T. J. Wang³⁹, W. Wang⁵⁴, W. H. Wang⁷¹, W. P. Wang^{66,53}, X. Wang^{42,g}, X. F. Wang^{34,j,k}, X. L. Wang^{10,f}, Y. Wang⁵⁶, Y. D. Wang⁴¹, Y. F. Wang^{1,53,58}, Y. H. Wang⁴³, Y. Q. Wang¹, Yaqian Wang^{16,1}, Z. Wang^{1,53}, Z. Y. Wang^{1,58}, Ziyi Wang⁵⁸, D. H. Wei¹³, F. Weidner⁶³, S. P. Wen¹, D. J. White⁶², U. Wiedner⁴, G. Wilkinson⁶⁴, M. Wolke⁷⁰, L. Wollenberg⁴, J. F. Wu^{1,58}, L. H. Wu¹, L. J. Wu^{1,58}, X. Wu^{10,f}, X. H. Wu³⁰, Y. Wu⁶⁶, Y. J Wu²⁸, Z. Wu^{1,53}, L. Xia^{66,53}, T. Xiang^{42,g}, D. Xiao^{34,j,k}, G. Y. Xiao³⁸, H. Xiao^{10,f}, S. Y. Xiao¹, Y. L. Xiao^{10,f}, Z. J. Xiao³⁷, C. Xie³⁸, X. H. Xie^{42,g}, Y. Xie⁴⁵, Y. G. Xie^{1,53}, Y. H. Xie⁶, Z. P. Xie^{66,53}, T. Y. Xing^{1,58}, C. F. Xu¹, C. J. Xu⁵⁴, G. F. Xu¹, H. Y. Xu⁶¹, Q. J. Xu¹⁵, X. P. Xu⁵⁰, Y. C. Xu⁵⁸, Z. P. Xu³⁸, F. Yan^{10,f}, L. Yan^{10,f}, W. B. Yan^{66,53}, W. C. Yan⁷⁵, H. J. Yang^{46,e}, H. L. Yang³⁰, H. X. Yang¹, L. Yang⁴⁷, S. L. Yang⁵⁸, Tao Yang¹, Y. F. Yang³⁹, Y. X. Yang^{1,58}, Yifan Yang^{1,58}, M. Ye^{1,53}, M. H. Ye⁸, J. H. Yin¹, Z. Y. You⁵⁴, B. X. Yu^{1,53,58}, C. X. Yu³⁹, G. Yu^{1,58}, T. Yu⁶⁷, X. D. Yu^{42,g}, C. Z. Yuan^{1,58}, L. Yuan², S. C. Yuan¹, X. Q. Yuan¹, Y. Yuan^{1,58}, Z. Y. Yuan⁵⁴, C. X. Yue³⁵, A. A. Zafar⁶⁸, F. R. Zeng⁴⁵, X. Zeng⁶, Y. Zeng^{23,h}, Y. H. Zhan⁵⁴, A. Q. Zhang¹, B. L. Zhang¹, B. X. Zhang¹, D. H. Zhang³⁹, G. Y. Zhang¹⁸, H. Zhang⁶⁶, H. H. Zhang⁵⁴, H. H. Zhang³⁰, H. Y. Zhang^{1,53}, J. L. Zhang⁷², J. Q. Zhang³⁷, J. W. Zhang^{1,53,58}, J. X. Zhang^{34,j,k}, J. Y. Zhang¹, J. Z. Zhang^{1,58}, Jianyu Zhang^{1,58}, Jiawei Zhang^{1,58}, L. M. Zhang⁵⁶, L. Q. Zhang⁵⁴, Lei Zhang³⁸, P. Zhang¹, Q. Y. Zhang^{35,75}, Shuihan Zhang^{1,58}, Shulei Zhang^{23,h}, X. D. Zhang⁴¹, X. M. Zhang¹, X. Y. Zhang⁵⁰, X. Y. Zhang⁴⁵, Y. Zhang⁶⁴, Y. T. Zhang⁷⁵, Y. H. Zhang^{1,53}, Yan Zhang^{66,53}, Yao Zhang¹, Z. H. Zhang¹, Z. Y. Zhang⁷¹, Z. Y. Zhang³⁹, G. Zhao¹, J. Zhao³⁵, J. Y. Zhao^{1,58}, J. Z. Zhao^{1,53}, Lei Zhao^{66,53}, Ling Zhao¹, M. G. Zhao³⁹, Q. Zhao¹, S. J. Zhao⁷⁵, Y. B. Zhao^{1,53}, Y. X. Zhao^{28,58}, Z. G. Zhao^{66,53}, A. Zhemchugov^{32,a}, B. Zheng⁶⁷, J. P. Zheng^{1,53}, Y. H. Zheng⁵⁸, B. Zhong³⁷, C. Zhong⁶⁷, X. Zhong⁵⁴, H. Zhou⁴⁵, L. P. Zhou^{1,58}, X. Zhou⁷¹, X. K. Zhou⁵⁸, X. R. Zhou^{66,53}, X. Y. Zhou³⁵, Y. Z. Zhou^{10,f}, J. Zhu³⁹, K. Zhu¹, K. J. Zhu^{1,53,58}, L. X. Zhu⁵⁸, S. H. Zhu⁶⁵, S. Q. Zhu³⁸, T. J. Zhu⁷², W. J. Zhu^{10,f}, Y. C. Zhu^{66,53}, Z. A. Zhu^{1,58}, B. S. Zou¹, J. H. Zou¹

¹ *Institute of High Energy Physics, Beijing 100049, People's Republic of China*

- ² *Beihang University, Beijing 100191, People's Republic of China*
- ³ *Beijing Institute of Petrochemical Technology, Beijing 102617, People's Republic of China*
- ⁴ *Bochum Ruhr-University, D-44780 Bochum, Germany*
- ⁵ *Carnegie Mellon University, Pittsburgh, Pennsylvania 15213, USA*
- ⁶ *Central China Normal University, Wuhan 430079, People's Republic of China*
- ⁷ *Central South University, Changsha 410083, People's Republic of China*
- ⁸ *China Center of Advanced Science and Technology, Beijing 100190, People's Republic of China*
- ⁹ *COMSATS University Islamabad, Lahore Campus, Defence Road, Off Raiwind Road, 54000 Lahore, Pakistan*
- ¹⁰ *Fudan University, Shanghai 200433, People's Republic of China*
- ¹¹ *G.I. Budker Institute of Nuclear Physics SB RAS (BINP), Novosibirsk 630090, Russia*
- ¹² *GSI Helmholtzcentre for Heavy Ion Research GmbH, D-64291 Darmstadt, Germany*
- ¹³ *Guangxi Normal University, Guilin 541004, People's Republic of China*
- ¹⁴ *Guangxi University, Nanning 530004, People's Republic of China*
- ¹⁵ *Hangzhou Normal University, Hangzhou 310036, People's Republic of China*
- ¹⁶ *Hebei University, Baoding 071002, People's Republic of China*
- ¹⁷ *Helmholtz Institute Mainz, Staudinger Weg 18, D-55099 Mainz, Germany*
- ¹⁸ *Henan Normal University, Xinxiang 453007, People's Republic of China*
- ¹⁹ *Henan University of Science and Technology, Luoyang 471003, People's Republic of China*
- ²⁰ *Henan University of Technology, Zhengzhou 450001, People's Republic of China*
- ²¹ *Huangshan College, Huangshan 245000, People's Republic of China*
- ²² *Hunan Normal University, Changsha 410081, People's Republic of China*
- ²³ *Hunan University, Changsha 410082, People's Republic of China*
- ²⁴ *Indian Institute of Technology Madras, Chennai 600036, India*
- ²⁵ *Indiana University, Bloomington, Indiana 47405, USA*
- ²⁶ *INFN Laboratori Nazionali di Frascati , (A)INFN Laboratori Nazionali di Frascati, I-00044, Frascati, Italy; (B)INFN Sezione di Perugia, I-06100, Perugia, Italy; (C)University of Perugia, I-06100, Perugia, Italy*
- ²⁷ *INFN Sezione di Ferrara, (A)INFN Sezione di Ferrara, I-44122, Ferrara, Italy; (B)University of Ferrara, I-44122, Ferrara, Italy*
- ²⁸ *Institute of Modern Physics, Lanzhou 730000, People's Republic of China*
- ²⁹ *Institute of Physics and Technology, Peace Avenue 54B, Ulaanbaatar 13330, Mongolia*
- ³⁰ *Jilin University, Changchun 130012, People's Republic of China*
- ³¹ *Johannes Gutenberg University of Mainz, Johann-Joachim-Becher-Weg 45, D-55099 Mainz, Germany*
- ³² *Joint Institute for Nuclear Research, 141980 Dubna, Moscow region, Russia*
- ³³ *Justus-Liebig-Universitaet Giessen, II. Physikalisches Institut, Heinrich-Buff-Ring 16, D-35392 Giessen, Germany*
- ³⁴ *Lanzhou University, Lanzhou 730000, People's Republic of China*
- ³⁵ *Liaoning Normal University, Dalian 116029, People's Republic of China*
- ³⁶ *Liaoning University, Shenyang 110036, People's Republic of China*
- ³⁷ *Nanjing Normal University, Nanjing 210023, People's Republic of China*
- ³⁸ *Nanjing University, Nanjing 210093, People's Republic of China*

- ³⁹ *Nankai University, Tianjin 300071, People's Republic of China*
- ⁴⁰ *National Centre for Nuclear Research, Warsaw 02-093, Poland*
- ⁴¹ *North China Electric Power University, Beijing 102206, People's Republic of China*
- ⁴² *Peking University, Beijing 100871, People's Republic of China*
- ⁴³ *Qufu Normal University, Qufu 273165, People's Republic of China*
- ⁴⁴ *Shandong Normal University, Jinan 250014, People's Republic of China*
- ⁴⁵ *Shandong University, Jinan 250100, People's Republic of China*
- ⁴⁶ *Shanghai Jiao Tong University, Shanghai 200240, People's Republic of China*
- ⁴⁷ *Shanxi Normal University, Linfen 041004, People's Republic of China*
- ⁴⁸ *Shanxi University, Taiyuan 030006, People's Republic of China*
- ⁴⁹ *Sichuan University, Chengdu 610064, People's Republic of China*
- ⁵⁰ *Soochow University, Suzhou 215006, People's Republic of China*
- ⁵¹ *South China Normal University, Guangzhou 510006, People's Republic of China*
- ⁵² *Southeast University, Nanjing 211100, People's Republic of China*
- ⁵³ *State Key Laboratory of Particle Detection and Electronics, Beijing 100049, Hefei 230026, People's Republic of China*
- ⁵⁴ *Sun Yat-Sen University, Guangzhou 510275, People's Republic of China*
- ⁵⁵ *Suranaree University of Technology, University Avenue 111, Nakhon Ratchasima 30000, Thailand*
- ⁵⁶ *Tsinghua University, Beijing 100084, People's Republic of China*
- ⁵⁷ *Turkish Accelerator Center Particle Factory Group, (A)Istinye University, 34010, Istanbul, Turkey; (B)Near East University, Nicosia, North Cyprus, Mersin 10, Turkey*
- ⁵⁸ *University of Chinese Academy of Sciences, Beijing 100049, People's Republic of China*
- ⁵⁹ *University of Groningen, NL-9747 AA Groningen, The Netherlands*
- ⁶⁰ *University of Hawaii, Honolulu, Hawaii 96822, USA*
- ⁶¹ *University of Jinan, Jinan 250022, People's Republic of China*
- ⁶² *University of Manchester, Oxford Road, Manchester, M13 9PL, United Kingdom*
- ⁶³ *University of Muenster, Wilhelm-Klemm-Strasse 9, 48149 Muenster, Germany*
- ⁶⁴ *University of Oxford, Keble Road, Oxford OX13RH, United Kingdom*
- ⁶⁵ *University of Science and Technology Liaoning, Anshan 114051, People's Republic of China*
- ⁶⁶ *University of Science and Technology of China, Hefei 230026, People's Republic of China*
- ⁶⁷ *University of South China, Hengyang 421001, People's Republic of China*
- ⁶⁸ *University of the Punjab, Lahore-54590, Pakistan*
- ⁶⁹ *University of Turin and INFN, (A)University of Turin, I-10125, Turin, Italy; (B)University of Eastern Piedmont, I-15121, Alessandria, Italy; (C)INFN, I-10125, Turin, Italy*
- ⁷⁰ *Uppsala University, Box 516, SE-75120 Uppsala, Sweden*
- ⁷¹ *Wuhan University, Wuhan 430072, People's Republic of China*
- ⁷² *Xinyang Normal University, Xinyang 464000, People's Republic of China*
- ⁷³ *Yunnan University, Kunming 650500, People's Republic of China*
- ⁷⁴ *Zhejiang University, Hangzhou 310027, People's Republic of China*
- ⁷⁵ *Zhengzhou University, Zhengzhou 450001, People's Republic of China*

^a *Also at the Moscow Institute of Physics and Technology, Moscow 141700, Russia*

^b *Also at the Novosibirsk State University, Novosibirsk, 630090, Russia*

^c Also at the NRC "Kurchatov Institute", PNPI, 188300, Gatchina, Russia

^d Also at Goethe University Frankfurt, 60323 Frankfurt am Main, Germany

^e Also at Key Laboratory for Particle Physics, Astrophysics and Cosmology, Ministry of Education; Shanghai Key Laboratory for Particle Physics and Cosmology; Institute of Nuclear and Particle Physics, Shanghai 200240, People's Republic of China

^f Also at Key Laboratory of Nuclear Physics and Ion-beam Application (MOE) and Institute of Modern Physics, Fudan University, Shanghai 200443, People's Republic of China

^g Also at State Key Laboratory of Nuclear Physics and Technology, Peking University, Beijing 100871, People's Republic of China

^h Also at School of Physics and Electronics, Hunan University, Changsha 410082, China

ⁱ Also at Guangdong Provincial Key Laboratory of Nuclear Science, Institute of Quantum Matter, South China Normal University, Guangzhou 510006, China

^j Also at Frontiers Science Center for Rare Isotopes, Lanzhou University, Lanzhou 730000, People's Republic of China

^k Also at Lanzhou Center for Theoretical Physics, Lanzhou University, Lanzhou 730000, People's Republic of China

^l Also at the Department of Mathematical Sciences, IBA, Karachi , Pakistan